NeuroImage: Clinical 17 (2018) 616–627

Contents lists available at ScienceDirect

NeuroImage: Clinical

journal homepage: www.elsevier.com/locate/ynicl

# Investigating structural and perfusion deficits due to repeated head trauma in active professional fighters

Virendra Mishra*, Karthik Sreenivasan, Sarah J. Banks, Xiaowei Zhuang, Zhengshi Yang, Dietmar Cordes, Charles Bernick

*Lou Ruvo Center for Brain Health, Cleveland Clinic Foundation, Las Vegas, NV, United States*

ARTICLE INFO

*Keywords:*
Repeated head trauma
Cerebral blood flow
Cognitive impairment
Neurovascular coupling
Brain morphology

ABSTRACT

Repeated head trauma experienced by active professional fighters results in various structural, functional and perfusion damage. However, whether there are common regions of structural and perfusion damage due to fighting and whether these structural and perfusion differences are associated with neuropsychological measurements in active professional fighters is still unknown. To that end, T1-weighted and pseudocontinuous arterial spin labeling MRI on a group of healthy controls and active professional fighters were acquired. Voxelwise group comparisons, in a univariate and multivariate sense, were performed to investigate differences in gray and white matter density (GMD, WMD) and cerebral blood flow (CBF) between the two groups. A significantly positive association between global GMD and WMD was obtained with psychomotor speed and reaction time, respectively, in our cohort of active professional fighters. In addition, regional WMD deficit was observed in a cluster encompassing bilateral pons, hippocampus, and thalamus in fighters (0.49 ± 0.04 arbitrary units (a.u.)) as compared to controls (0.51 ± 0.05a.u.). WMD in the cluster of active fighters was also significantly associated with reaction time. Significantly lower CBF was observed in right inferior temporal lobe with both partial volume corrected (46.9 ± 14.93 ml/100 g/min) and non-partial volume corrected CBF maps (25.91 ± 7.99 ml/100 g/min) in professional fighters, as compared to controls (65.45 ± 22.24 ml/100 g/min and 35.22 ± 12.18 ml/100 g/min respectively). A paradoxical increase in CBF accompanying right cerebellum and fusiform gyrus in the active professional fighters (29.52 ± 13.03 ml/100 g/min) as compared to controls (19.43 ± 12.56 ml/100 g/min) was observed with non-partial volume corrected CBF maps. Multivariate analysis with both structural and perfusion measurements found the same clusters as univariate analysis in addition to a cluster in right precuneus. Both partial volume corrected and non-partial volume corrected CBF of the cluster in the thalamus had a significantly positive association with the number of fights. In addition, GMD of the cluster in right precuneus was significantly associated with psychomotor speed in our cohort of active professional fighters. Our results suggest a heterogeneous pattern of structural and CBF deficits due to repeated head trauma in active professional fighters. This finding indicates that investigating both structural and CBF changes in the same set of participants may help to understand the pathophysiology and progression of cognitive decline due to repeated head trauma.

## 1. Introduction

Sports-related traumatic brain injuries (TBI) amount to 21% of total TBI in the USA of which 5% of the cases are due to professional fighting (http://www.cpsc.gov/en/Research–Statistics/NEISS-Injury-Data/) (Langlois et al., 2006). Repeated head trauma, as experienced by professional fighters, has been indicated as a risk factor for neurodegenerative disorders such as dementia and various other neuropsychiatric disorders such as depression, and mood disorders (For review: Bazarian et al., 2009; Bigler, 2013; Jordan, 2013). Some individuals with chronic brain injury due to repeated head trauma have shown evidence of chronic traumatic encephalopathy (CTE) at autopsy (For review: McKee et al., 2013; Victoroff, 2013). Neuropsychological testing in boxers has revealed slower processing speed, difficulty in completing complex attentional tasks and reduction in executive functions (Bernick and Banks, 2013; Heilbronner et al., 2009). The exact pathophysiology is, however, difficult to investigate due to inherent heterogeneity among the subjects due to different injury sites, mechanical forces, and exposure to head trauma (Margulies and Hicks, 2009; Xiong et al., 2013).

Both structural and perfusion deficits have been found in animals

* Corresponding author at: Cleveland Clinic Lou Ruvo Center for Brain Health, 888 W. Bonneville Avenue, Las Vegas, NV 89106, United States.
*E-mail address:* mishrav@ccf.org (V. Mishra).

https://doi.org/10.1016/j.nicl.2017.11.013
Received 19 April 2017; Received in revised form 13 November 2017; Accepted 14 November 2017
Available online 21 November 2017

and human models of repeated head trauma. The animal models of repeated head trauma have reported widespread cortical, cerebellar, hippocampal, and thalamic atrophy combined with diffuse axonal injuries of the corpus callosum and cerebellar peduncles (Xiong et al., 2013; (review)). Similar to these animal models, various structural neuroimaging studies of repeated head trauma in humans involved in repeated head trauma such as professional fighting, veterans, and combatants have shown changes in gray matter volumes in regions such as thalamus, ventromedial prefrontal cortices, right fusiform gyrus, and frontotemporolimbic regions involving hippocampus, medial temporal lobe, and frontal lobes (Bernick et al., 2015; Bigler, 2013 (review); Gooijers et al., 2013; Lopez-Larson et al., 2013; Montenigro et al., 2015; Ng et al., 2014 (review)). Various diffusion tensor imaging (DTI) studies of repeated head trauma have shown increased mean diffusivity and decreased fractional anisotropy in the temporo-occipital white matter tracts and forceps major (Hulkower et al., 2013 (review); Ng et al., 2014 (review); Orrison et al., 2009 (review); Shin et al., 2014; Wintermark et al., 2015 (review); Zhang et al., 2003, 2006). Axonal diffuse injury, hippocampal atrophy, dilated perivascular spaces, cavum septum pellucidum, cerebral atrophy, increased lateral ventricular size, pituitary gland atrophy, arachnoid cysts, and contusions have been shown to be associated with repeated head injuries that were further associated with years and number of fights (Orrison et al., 2009 (review)). Perfusion studies using dynamic susceptibility contrast MRI, single photon emission computed tomography (SPECT) and arterial spin labeling (ASL) MRI in participants with repeated brain trauma has shown global perfusion deficits accompanied with lower cerebral blood flow in thalamus, cingulate gyri, cerebellum, cuneus and temporal lobes (For review: Eierud et al., 2014; Koerte et al., 2016). The perfusion deficit was further shown to be associated with neurocognitive scores (Ge et al., 2009; Koerte et al., 2016; Liu et al., 2013).

Therefore, there is an established association of both morphological and perfusion changes in fighters with repeated head trauma. However the extant neuroimaging studies in humans have investigated either structural or perfusion changes in fighters but not both in the same population. Jointly investigating both structural and perfusion changes may provide additional information about the pathophysiology and the progression of cognitive decline in participants with repeated head trauma. To that end, in the current study, we investigated both structural and perfusion changes in active professional fighters and their association with exposure to fighting and neuropsychological assessments. The data were collected as a part of Professional Fighters Brain Health Study (PFBHS) (Bernick et al., 2013). We hypothesized that repeated head trauma will induce (a) both global structural and perfusion deficits as compared to age and education-matched healthy controls, (b) there may be both overlapping and non-overlapping regions of structural and perfusion deficits due to repeated head trauma, and (c) the regions showing significant structural and perfusion deficits as compared to healthy controls will be associated with both exposure to fighting and neuropsychological assessments.

## 2. Materials and methods

PFBHS is a longitudinal study of active professional fighters (boxers and MMA) and age and education-matched healthy controls (Bernick et al., 2013). PFBHS was approved by the institutional review board of Cleveland Clinic and all the participants provided informed written consent. The protocols of the experiment were explained to all the subjects and were performed according to the Declaration of Helsinki guidelines and Belmont Report.

### 2.1. Active fighters and healthy controls recruitment and demographics

252 professional fighters (234 males (M); 18 females (F)) and 20 age-matched healthy controls (20M) were recruited at our centre. All subjects aged 18 or older licensed for professional boxing or mixed martial arts and who are fluent in English were included as professional fighters. Fighters competing in a sanctioned competition within 45 days of the visit were excluded. Control subjects could not have participated in contact sports such as rugby, football, hockey, soccer, or rodeo at the high school or above. There were 108 boxers (98M, 10F) and 144 MMA-fighters (136M, 8F). None of the fighters included for the purpose of this study suffered from hypertension, diabetes, or any other medical complications that may affect CBF measurements. All fighters who had concussion-like symptoms on the day of their visit were also excluded for the purpose of this study. Detailed information about race, educational attainment, prior involvement in other combat sports and professional fighting were recorded for most of the subjects (221 fighters, 20 controls).

Since both race and years of education (YOE) affect CBF values, those subjects that had missing information on either race (22 fighters), years of education (YOE) (seven fighters), or both race and YOE (two fighters) were removed from any further analysis. Furthermore, one control and seven fighters had registration and motion artifacts and were excluded from any analysis. This procedure yielded 19 healthy controls (19M), and 214 (14F, 200M) professional fighters (89 boxers (6F, 83M), and 125 MMA-fighters (8F, 117M)). Since there were no female controls, only male fighters and controls were used for this analysis. Therefore, 19 male healthy controls and 200 male professional fighters (83 boxers and 117 MMA-fighters) were used for the statistical analysis. Demographics of the groups are tabulated in Table 1.

### 2.2. Neuropsychological assessment

Cognitive tests were completed using a computer in a quiet room, supervised by a researcher. CNS Vital Signs was used to administer standardized cognitive tests (Gualtieri and Johnson, 2006). We use four tests from their battery; Finger Tapping, Symbol Digit Coding, Stroop and a Verbal Memory task involving list learning. From these tests we obtained four cognitive scores, namely verbal memory (total correct across immediate and delayed recognition tasks using a 15 item list), processing speed (total correct on a Digit Symbol Coding task), psychomotor speed (combining Digit Symbol result and average Finger Tapping on each hand) and reaction time (which uses the scores from the Stroop task) for all the participants. Table 2 tabulates the neuropsychological assessment scores.

### 2.3. MRI data acquisition

3T Verio Siemens MRI scanner with a 32-channel head coil was used

**Table 1**
Various demographics of all the participants are shown along with their mean ± SD. Results of pairwise statistical comparisons are also shown with their respective *p*-values. *p*-Values are represented by the letter "*p*". NS: Non-significant; NA: Not applicable.

| Demographics | Control ($N$ = 19) | Fighters ($N$ = 214) | Control vs fighters |
|---|---|---|---|
| Age (years) | 29 ± 7.53 | 28.98 ± 5.86 | NS ($p$ = 0.95) |
| Years of education (years) | 14.59 ± 2.67 | 13.71 ± 2.47 | NS ($p$ = 0.11) |
| Race | | | |
| Unknown: | 2 | 30 | |
| Pacific Islander: | 2 | 8 | |
| Asian: | 1 | 3 | |
| African American: | 1 | 56 | |
| American Indian/ Alaskan Native: | 0 | 3 | NS ($p$ = 0.15) |
| White: | 13 | 100 | |
| Number of professional fights | NA | 12.69 ± 12.16 | NA |
| Years of professional fights | NA | 5.18 ± 4.03 | NA |
| Number of knockouts | NA | 0.91 ± 1.53 | NA |

**Table 2**
Various neuropyschological assessment test results are shown along with their mean ± SD. Results of pairwise statistical comparisons are also shown with their respective *p*-values and effect size. *p*-Values are represented by the letter "*p*" and effect size is represented by letter "d". NS: Non-significant.

| Neuropsychological scores | Control ($N$ = 19) | Fighters ($N$ = 214) | Control vs fighters |
|---|---|---|---|
| Verbal memory | 53.21 ± 3.81 | 51.43 ± 4.91 | NS ($p$ = 0.11); d = 0.1 |
| Processing speed | 66.21 ± 15.75 | 52.47 ± 10.99 | $p$ < 0.001; d = 0.3 |
| Psychomotor speed | 199 ± 24.04 | 171.28 ± 22.95 | $p$ < 0.001; d = 0.3 |
| Reaction time | 660.42 ± 84.28 | 709.59 ± 100.32 | $p$ = 0.02; d = 0.16 |

to acquire the following MRI data for each subject. Structural T1-scan: 3D magnetization prepared rapid gradient echo (MPRAGE) T1 weighted scan was performed with: field of view (FOV) = 256 × 256 × 160; voxel size = 1 × 1 × 1.2 $mm^3$; TR = 2300 ms, TE = 2.98 ms; TI = 900 ms and flip angle = 9°. ASL-MRI (pCASL): pCASL sequence with 2D single-shot gradient-echo EPI was performed with: voxel size = 3.5 × 3.5 × 5 $mm^3$; TR = 4500 ms; labeling duration = 1500 ms; post labeling delay = 1200 ms; TE = 29 ms; FOV = 224 × 224 $mm^2$; number of slices = 29; number of dynamics = 100 with 50 control and tag pairs. Both the scans were performed in the same session. Total imaging scan time was 15 min.

### 2.4. Image processing and analysis

Image processing was performed using SPM12 (http://www.fil.ion.ucl.ac.uk/spm/software/spm12/), FreeSurfer v5.3.0 (http://surfer.nmr.mgh.harvard.edu/), FSL v5.0.9 (http://fsl.fmrib.ox.ac.uk/fsl/fslwiki/) and Matlab® 2015a (http://www.mathworks.com/help/matlab/).

#### 2.4.1. Voxel-based morphometry (VBM) analysis

VBM analysis to compare modulated gray matter and white matter density between controls and fighters were performed using Diffeomorphic Anatomical Registration Through Exponential Lie Algebra (DARTEL) toolbox (Ashburner, 2007). Briefly, the steps can be summarized as follows: (1) T1-weighted images are segmented using standard unified segmentation model in SPM12 to produce gray matter (GM), white matter (WM), and cerebrospinal fluid (CSF) probability maps in MNI152 space; (2) the study-specific GM and WM templates were created from the segmented GM and WM images by randomly selecting the same number of fighters as controls to stay unbiased to population distribution; (3) an initial affine registration of both GM and WM templates to tissue probability maps in MNI152 space was then performed; (4) both affine registered GM and WM templates were nonlinearly warped to GM and WM templates in MNI152 space respectively, and were used in the modulation step in order to ensure that the relative volumes of GM and WM were preserved following the spatial normalization (2 $mm^3$ isotropic resolution) by the Jacobian determinant of the deformation field; and (5) spatial smoothing was finally performed on the modulated and normalized GM and WM images with a 8 mm full width at half maximum (FWHM) isotropic Gaussian kernel and were used to statistically compare modulated GM density (GMD) and WMD between the two groups. WMD obtained using DARTEL encompasses both the white matter and the subcortical brain regions.

#### 2.4.2. CBF quantification

ASL data was first motion corrected using MCFLIRT in FSL for the control and label image series separately (Jenkinson et al., 2002; Wang et al., 2008). The perfusion map of every subject was calculated using Variational Bayesian approach (Chappell et al., 2009) using BASIL toolbox (as a part of the FMRIB Software Library https://fsl.fmrib.ox.ac.uk/fsl/fslwiki/BASIL). BASIL toolbox estimates perfusion according to the single well-mixed compartment of Buxton et al. (Buxton et al., 1998). Voxelwise calibrated CBF image for every subject was obtained by dividing the relative perfusion map by the voxelwise calibration. Voxelwise calibration (Alsop et al., 2015) was performed including the bias field map and correction for partition coefficient and the labeling efficiency. The bias field map was obtained by segmenting the T1-weighted image using FAST toolbox in FSL (Zhang et al., 2001), and was used as an approximate of the coil sensitivity map. The other parameters used in the Bayesian inference using the Buxton model (Buxton et al., 1998) were as follows: labeling efficiency (0.85 for pCASL) (Wu et al., 2007), blood-brain barrier coefficient (0.9 ml/g) (Herscovitch and Raichle, 1985), bolus duration (1.5 s), delay between the end of labeling and the start of the acquisition (1.2 s), and the longitudinal relaxation time of the brain tissue (1.65 s) at 3T (Lu et al., 2004). An adaptive spatial prior was used to smooth the estimated perfusion map to exploit the spatial homogeneity of the perfusion map without interacting with non-linear kinetic curve modelling.

All statistical comparisons were performed on the smoothed calibrated CBF images in the standard space. The procedure to generate smoothed calibrated CBF images for each subject in the standard space is as follows. First, the mean ASL control image was registered to the high-resolution T1 image and the transformation was applied to the calibrated CBF map. Then, the anatomical scan was spatially normalized to the MNI152 template (2 $mm^3$) using SPM12's unified segmentation normalization tool (http://www.fil.ion.ucl.ac.uk/spm/software/spm12/) in order to perform group-wise statistical comparisons. Then, the transformation matrix was applied to registered calibrated CBF map to obtain spatially normalized CBF maps in MNI152 standard space. All the spatially normalized CBF maps were averaged with a Gaussian filter (FWHM = 4 mm) before statistical comparison.

Since the low resolution of the ASL maps can interfere with the accuracy of CBF quantification, partial volume corrected CBF maps (CBF-PV-Corr) for each subject in their individual native space were also generated according to the procedure outlined in Chen et al. (Chen et al., 2011). Briefly, high-resolution GM and WM probability maps were subsampled to the resolution of the ASL images and thresholded to 0.3 to minimize division artifacts before being applied to the non-partial volume corrected CBF maps (CBF-NonPV-Corr) obtained in the previous paragraph. CBF-PV-Corr maps were computed using the equation:

$$\mathrm{CBF-PV-Corr} = \frac{\mathrm{CBF-NonPV-Corr}}{\mathrm{P_{GM}} + 0.4{*}\mathrm{P_{WM}}}$$

where 0.4 is the global ratio between GM and WM (Du et al., 2006), and $P_{GM}$ and $P_{WM}$ are the probabilities of GM and WM in every voxel respectively. The procedure outlined in the previous paragraph for CBF-NonPV-Corr map was repeated for CBF-PV-Corr maps to spatially normalize each subject's CBF-PV-Corr map to MNI152 space and were averaged with a Gaussian filter (FWHM = 4 mm) before statistical comparison. All the individual CBF-PV-Corr and CBF-NonPV-Corr maps were inspected for obvious arterial artifacts.

Whole brain mask was generated for every subject in the native space. The high-resolution T1 image was registered to the mean ASL control image and the transformation was applied to the GM and WM probability map. A binary whole brain mask was finally obtained by assigning 1 to all voxels where sum of the individual GM and WM probabilities was equal to 1, and 0 otherwise. This whole brain mask was applied to the CBF-PV-Corr and CBF-NonPV-Corr map and a single value of mean whole brain CBF-PV-Corr and CBF-NonPV-Corr were obtained for each subject which was used as a regressor to remove subject level global differences in perfusion between individuals.

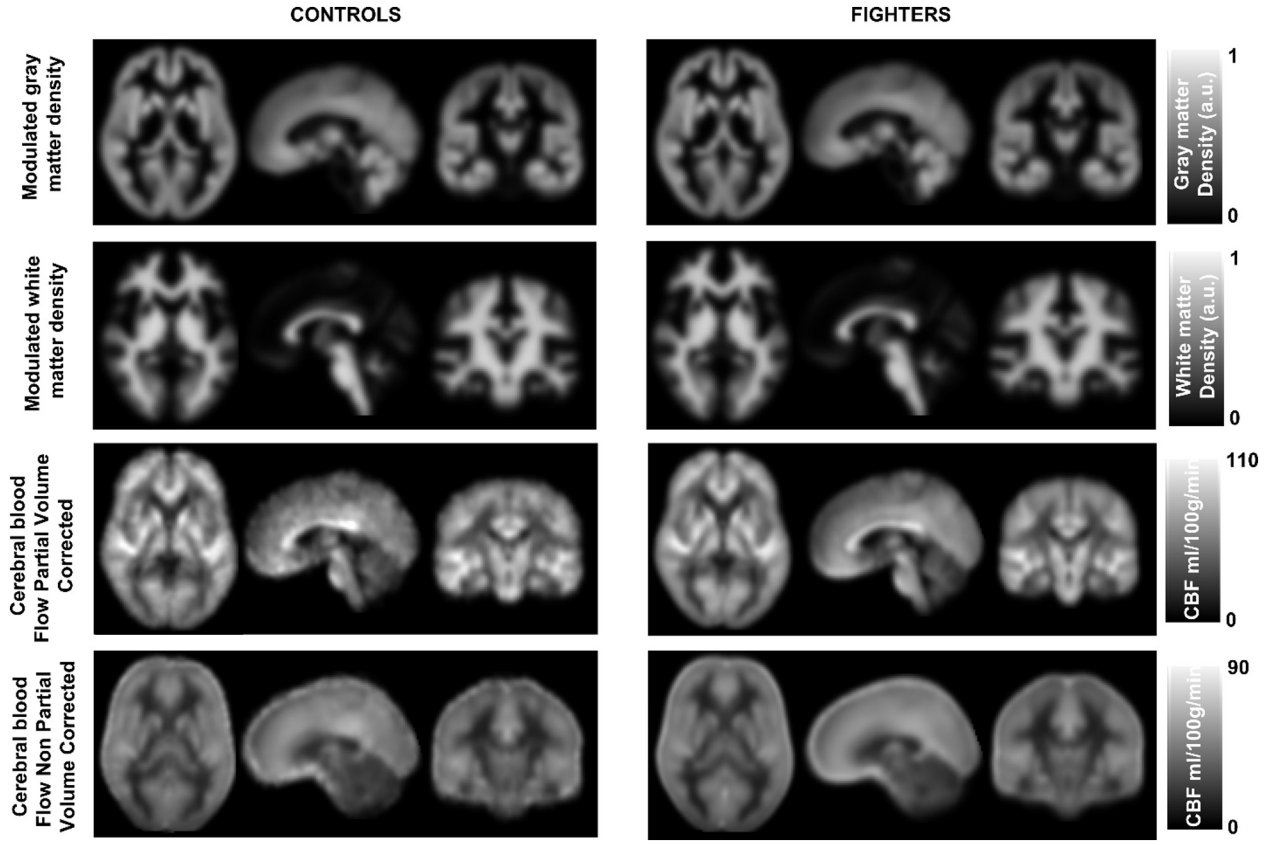


**Fig. 1.** Mean modulated gray matter density (GMD), modulated white matter density (WMD), and partial volume corrected cerebral blood flow (CBF), and non-partial volume corrected CBF in MNI space shown for healthy controls (left panel) and fighters (right panel) in all the three orientations. The color bar represent the range of GMD (arbitrary units (a.u.)), WMD (a.u.), and CBF (ml/100 g/min).

### 2.4.3. Multivariate GMD, WMD, and CBF analysis

A joint analysis of GMD and WMD with both CBF-PV-Corr and CBF-NonPV-Corr maps was conducted using a modified nonparametric combination implemented in PALM toolbox in FSL (Winkler et al., 2016) to investigate if there are any overlapping regions of structural and perfusion deficits due to repeated head trauma, and whether the regions showing significant structural and perfusion deficits as compared to healthy controls are associated with both exposure to fighting and neuropsychological assessments.

## 2.5. Statistical analysis

Two sample *t*-test was performed in SPM12 to assess group differences in modulated GMD, WMD, CBF-PV-Corr, and CBF-NonPV-Corr between control and fighters. Age, gender, years of education, race, global CBF, type of fighting style (boxing or MMA), and intracranial volume were used as nuisance regressor as they may modulate both CBF and morphological structures (Good et al., 2001; Hanyu et al., 2008; Leenders et al., 1990; Liu et al., 2016). The t-maps were thresholded with a cluster defining a threshold (CDT) of voxel-wise uncorrected $p < 0.001$ resulting in a cluster-extent threshold of $k \geq 377$, $k \geq 328$, $k \geq 104$, and $k \geq 164$ for GMD, WMD, and CBF-PV-Corr and CBF-NonPV-Corr respectively to achieve a cluster-level family-wise error rate (FWER) of 0.05. Various cluster sizes were obtained for the comparisons at the same uncorrected $p < 0.001$ as the smoothness estimate to satisfy assumptions of random field theory (Worsley et al., 1996) were different for each group comparisons. FWHM were [9.86, 12.49, 11.56] mm, [12.34, 14.67, 13.62] mm, [9.99, 11.79, 9.45] mm, and [12.1, 14.93, 11.84] mm for GMD, WMD, CBF-PV-Corr and CBF-NonPV-Corr comparisons respectively. Cohen's effect size (d) was calculated for each significant clusters. GMD, WMD, CBF-PV-Corr and CBF-NonPV-Corr were extracted in the significantly different clusters for each subject and the relationship between GMD, WMD, CBF-PV-Corr, and CBF-NonPV-Corr and various neuropsychological tests along with the exposure to fighting were assessed controlling for the nuisance regressor, stated above. The relationship was corrected for multiple comparisons between the clusters using PALM toolbox in FSL (Winkler et al., 2016) and *Cohen's d* was calculated for each significant relationship since multiple linear regression analysis was used in this study. Only FWER *p*-values are reported wherever applicable.

FWER of 0.05 was considered significant for joint analysis using a modified nonparametric combination. As before, GMD and WMD along with CBF-PV-Corr or CBF-NonPV-Corr were extracted in the significantly different clusters for each subject and the relationship between GMD, WMD, CBF-PV-Corr, or CBF-NonPV-Corr and various neuropsychological tests along with the exposure to fighting were assessed controlling for the nuisance regressor, stated above. The relationship was corrected for multiple comparisons between the clusters using PALM toolbox in FSL (Winkler et al., 2016) and *Cohen's d* was calculated for each significant relationship. Only FWER *p*-values are reported wherever applicable.

Chi-square ($\chi^2$) test was conducted to check significance for categorical demographic variables and Wilcoxon rank sum test was conducted to check for statistical significance of continuous demographic variables and neuropsychological scores. Significance was established at $p < 0.05$ and the results were reported as mean ± standard deviation (SD) along with their associated effect size, wherever applicable.

## 3. Results

### 3.1. Demographics and clinical scores

Tables 1 and 2 outlines the descriptive statistics as mean ± SD, *p*-values and the associated effect sizes, for the demographics and the cognitive assessment scores, between the two groups.

None of the demographics such as age, YOE, and race was significantly different between the groups (Table 1). As would be expected, there were several differences in cognitive scores between the groups (Table 2). Fighters had significantly worse processing speed ($p < 10^{-3}$; d = 0.3), psychomotor speed ($p < 10^{-3}$; d = 0.3), and reaction time ($p = 0.02$; d = 0.16) when compared to controls. Verbal memory was found to be non-significant between controls and fighters.

### 3.2. Global effects of repeated head trauma on both structural and CBF measurements

Both controls and fighters had a similar range of mean GMD, WMD, CBF-PV-Corr and CBF-NonPV-Corr as shown in Fig. 1. Whole brain (global) GMD (modulated), WMD (modulated), CBF-PV-Corr and CBF-NonPV-Corr were estimated to be 0.43 ± 0.11 (arbitrary units (a.u.)), 0.49 ± 0.16a.u., 53.08 ± 15.88 ml/100 g/min, and 37.31 ± 7.15 ml/100 g/min in controls and 0.43 ± 0.1a.u., 0.48 ± 0.15a.u., 51.05 ± 14.27 ml/100 g/min and 36.84 ± 6.74 ml/100 g/min in fighters respectively. Fig. 2 shows the association of GMD and WMD with neuropsychological assessment scores. A significantly positive association was observed between psychomotor speed and global GMD ($p = 0.01$, d = 0.17) in the fighters cohort. Fighters also showed a negative association ($p = 0.03$, d = 0.17) with reaction time and WMD due to repetitive head trauma. No other measurements showed any associations with either global structural or global CBF measurements.

### 3.3. Regional effects of repeated head trauma on structural MRI measurements

Only one cluster was found to have lower modulated WMD in active professional fighters (0.49 ± 0.04 a.u.) as compared to healthy controls (0.51 ± 0.05 a.u.). As shown in Fig. 3, the cluster was found to be predominantly located in the bilateral thalamus, hippocampus, and pons.

Also, as shown in Fig. 3, a significantly negative association was observed between modulated WMD of the cluster and reaction time in active professional fighters ($p = 0.02$, d = 0.17). None of the other neuropsychological measures or exposure to fighting had any association with any clusters in either group.

No significant difference was observed in regional modulated GMD between healthy controls and fighters.

### 3.4. Regional effects of repeated head trauma on CBF

As shown in Fig. 4, significantly lower CBF-PV-Corr was observed in the right inferior temporal lobe in fighters (46.9 ± 14.93 ml/100 g/min) as compared to controls (65.45 ± 22.24 ml/100 g/min). CBF-PV-Corr showed a significantly positive association with verbal memory ($p = 0.0054$, d = 0.21) in controls, as shown in Fig. 4. Also, as shown in Fig. 4, controls showed a significantly negative association between CBF-PV-Corr and reaction time ($p = 0.02$, d = 0.17).

The cluster in the right inferior temporal lobe was also present in the CBF-NonPV-Corr and had a significantly lower CBF-NonPV-Corr in fighters (25.91 ± 7.99 ml/100 g/min) as compared to controls (35.22 ± 12.18 ml/100 g/min), as shown in Fig. 5. Additionally, as shown in Fig. 5, there was a cluster encompassing right fusiform gyrus and cerebellum (cluster 2) which had a significantly higher CBF in fighters (29.52 ± 13.03 ml/100 g/min) as compared to controls (19.46 ± 12.56 ml/100 g/min). A similar association, as before, between CBF-NonPV-Corr was observed with verbal memory ($p < 0.001$, d = 0.32) and reaction time ($p = 0.007$, d = 0.17) in controls, as shown in Fig. 5. In addition, a significantly negative association was observed in healthy controls between CBF-NonPV-Corr and psychomotor speed ($p = 0.0068$, d = 0.2). None of the other neuropsychological measures or exposure to fighting had any association with any clusters in either group.

### 3.5. Multivariate analysis of GMD, WMD, and CBF measurements

Four clusters were found to be significantly different ($p < 0.05$) in fighters as compared to controls (Fig. 6) using modified NPC by combining modulated GMD, WMD, and CBF-PV-Corr. The clusters were located in the right precuneus (cluster 1), bilateral hippocampus (cluster 2 and cluster 3), and bilateral thalamus (cluster 4). Also, as shown in Fig. 6, modulated GMD in cluster 1 and CBF-PV-Corr in cluster 4 were found to be significantly positively associated with psychomotor speed ($p = 0.04$, d = 0.19) and numbers of fighting ($p = 0.03$, d = 0.2) respectively, in fighters as compared to controls.

When CBF-NonPV-Corr was combined with modulated GMD and WMD, five clusters were found to be significantly different in fighters as compared to controls (Fig. 7). The clusters were located in the right precuneus (cluster 1), right olfactory cortex (cluster 2), bilateral hippocampus (cluster 3 and cluster 4), and bilateral thalamus (cluster 5). Additionally, a similar relationship between modulated GMD in cluster 1 and CBF-PV-Corr in cluster 5 were found to be significantly positively associated with psychomotor speed ($p = 0.03$, d = 0.2) and numbers of fighting ($p = 0.007$, d = 0.25) in fighters as compared to controls.

Tables 3–5 show mean ± SD of GMD, WMD, CBF-PV-Corr, and CBF-NonPV-Corr in each group along with the number of voxels in each cluster and the effect size of the significant clusters. Table 6 summarizes our findings.

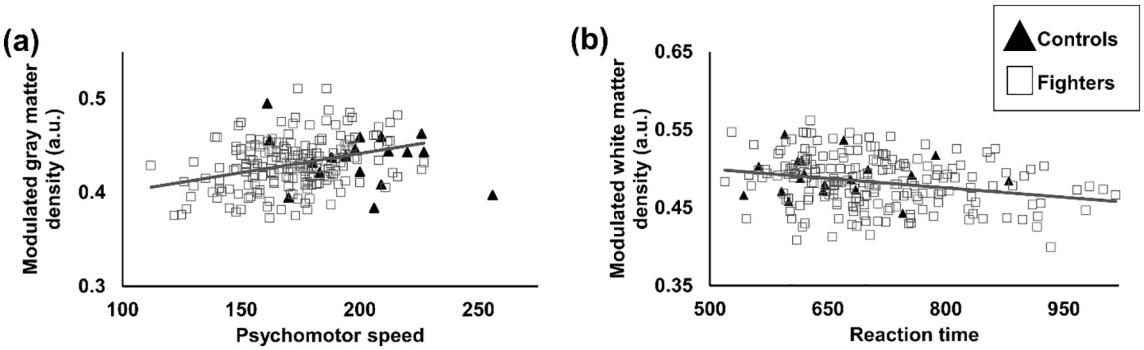


**Fig. 2.** (a) Scatterplot of modulated GMD is shown as a function of psychomotor speed. (b) Scatterplot of modulated WMD is shown as a function of reaction time. Every scatter represents global GMD and WMD for every subject. The regression line is shown for fighters in gray color. The regression line for controls is not shown as there was no association between the GMD and psychomotor speed or WMD and reaction time in our cohort of active professional fighters. *$p < 0.05$.

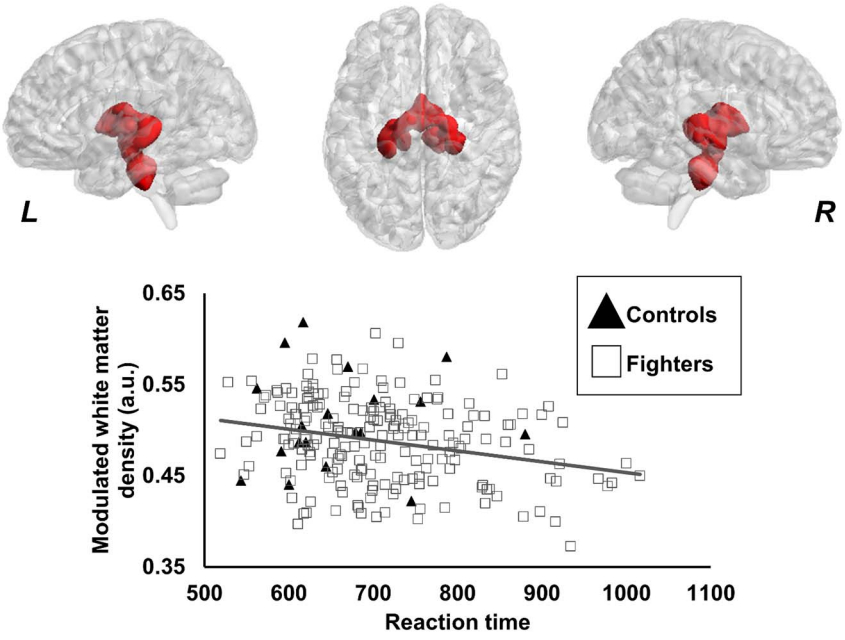


**Fig. 3.** Spatial location of the voxels where modulated WMD was lower in fighters as compared to healthy controls. The panel shows the 3D representation of the extent of the clusters from on MNI152 glass brain. L, R represents the left and right hemisphere. Scatterplot of modulated WMD is also shown as a function of reaction time. Every scatter represents WMD in the entire cluster for every subject. The regression line is shown for fighters in gray color. The regression line for controls is not shown as there was no association between the WMD and reaction time. *$p < 0.05$.

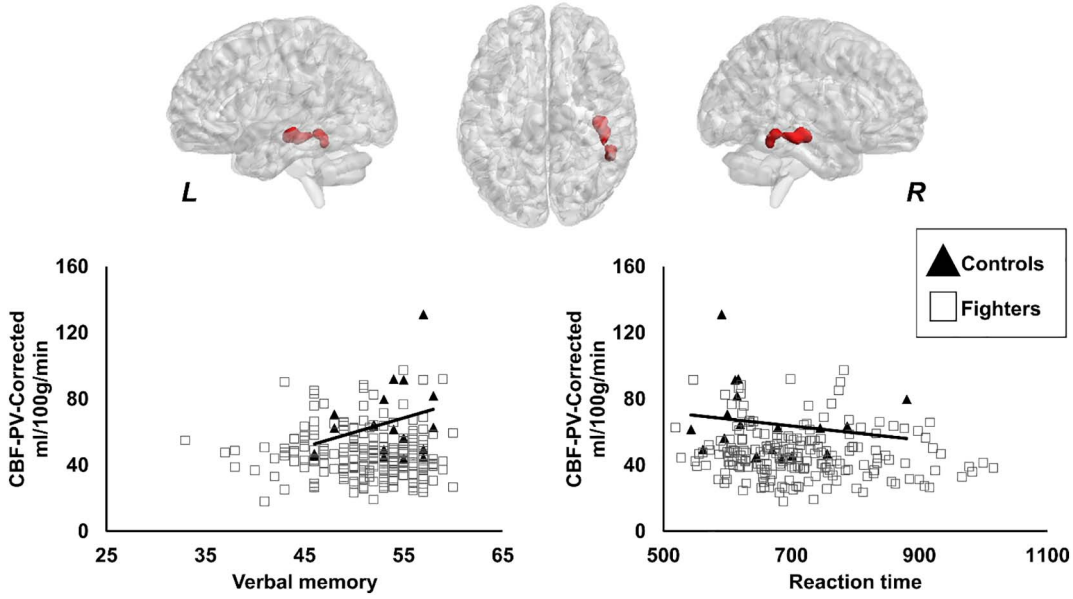


**Fig. 4.** Spatial location of the voxels where partial volume corrected cerebral blood flow (CBF-PV-Corr) was lower in fighters as compared to healthy controls. The panel shows the 3D representation of the extent of the clusters from on MNI152 glass brain. L, R represents the left and right hemisphere. Scatterplot of CBF-PV-Corr is also shown as a function of verbal memory and reaction time. Every scatter represents CBF-PV-Corr in the entire cluster for every subject. The regression line is shown for controls in black color. The regression line for fighters is not shown as there was no association between CBF-PV-Corr and verbal memory or CBF-PV-Corr and reaction time in our cohort of active professional fighters. *$p < 0.05$.

## 4. Discussion

Our findings in active professional fighters due to repeated head trauma suggests that: (a) there is no global deficit in GMD, WMD, CBF-PV-Corr, or CBF-NonPV-Corr, although, there was a positive association of both global GMD and WMD with psychomotor speed and reaction time in our cohort of active fighters, respectively; (b) WMD, CBF-PV-Corr, and CBF-NonPV-Corr deficits exists due to repeated head trauma similar to previous findings (Bigler, 2013 (review); Eierud et al., 2014 (review); Koerte et al., 2016 (review); Montenigro et al., 2015; Ng et al., 2014 (review); Orrison et al., 2009 (review); Wintermark et al., 2015 (review)); and (c) multivariate analysis combining GMD and WMD with CBF measurements (both PV-Corr and NonPV-Corr) revealed clusters where either structural or perfusion measurements were associated with exposure to fighting or neuropsychological assessments. Hence, our study suggests that repeated head trauma induces a complex pattern of structural and perfusion deficits, and both CBF and structural deficits should be investigated in the same set of subjects to better inform the clinical effects of repeated head trauma.

Repeated head blows due to fighting may cause neural tissue damage which has been shown to produce a cascade of either regional or global brain atrophy depending on the severity and type of injury (Bigler, 2013 (review); Blennow et al., 2012 (review); Davis, 2000 (review); Eierud et al., 2014 (review); Gooijers et al., 2013; Koerte et al., 2016 (review); Langlois et al., 2006 (review)). However, we did not find any global differences in structural or perfusion measurements although, both global GMD and WMD was significantly associated with psychomotor speed and reaction time, respectively, in active

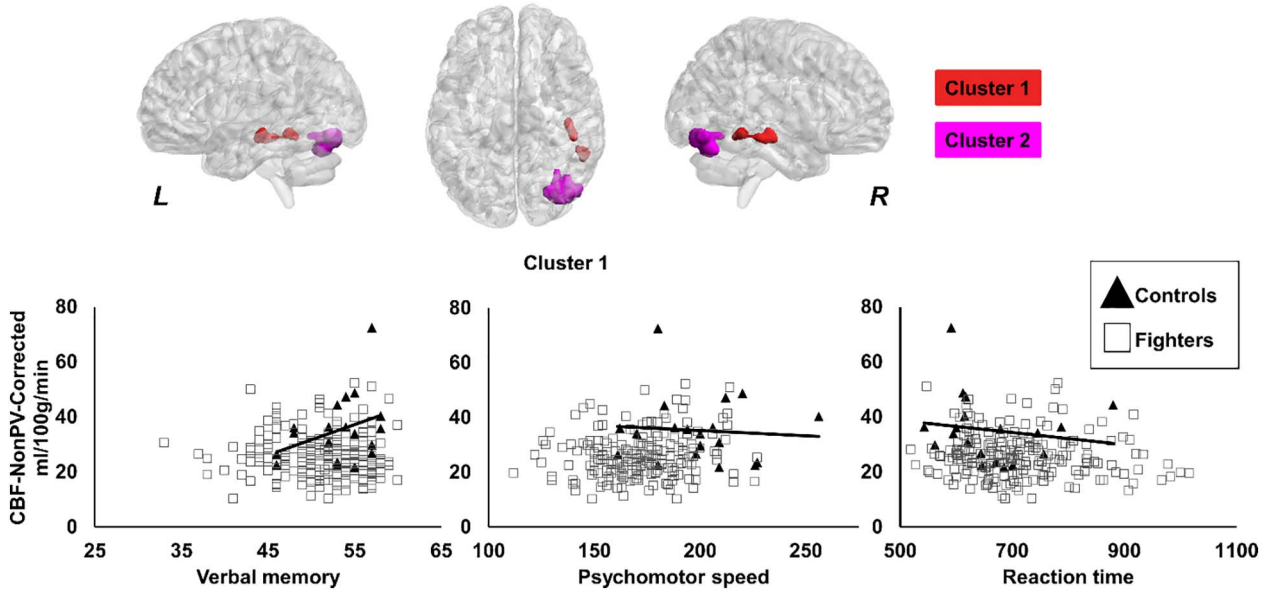


**Fig. 5.** Spatial location of the voxels where non-partial volume corrected cerebral blood flow (CBF-NonPV-Corr) was lower in fighters as compared to healthy controls. Cluster 1 and cluster 2 are shown in red and pink color respectively. The panel shows the 3D representation of the extent of the clusters from on MNI152 glass brain. L, R represents the left and right hemisphere. Scatterplot of CBF-NonPV-Corr is also shown as a function of verbal memory, psychomotor speed, and reaction time. Every scatter represents CBF-NonPV-Corr in the respective cluster for every subject. The regression line is shown for controls in black color. The regression line for fighters is not shown as there was no association between CBF-NonPV-Corr and verbal memory or CBF-NonPV-Corr and psychomotor speed or CBF-NonPV-Corr and reaction time in our cohort of active professional fighters. $*p < 0.05$. (For interpretation of the references to color in this figure legend, the reader is referred to the web version of this article.)

professional fighters. Our finding suggests that structural atrophy due to repeated head trauma may be associated with cognition similar to retired fighters (For review: Graham et al., 2014; McKee et al., 2009, 2013); and that structural measurement may be more sensitive than perfusion measurement on a global scale.

Lower thalamic volumes due to repeated head blows has been shown to be associated with poor cognitive functions (Bernick et al., 2015). Both hippocampal and thalamic atrophy have been widely reported in animal (Hall et al., 2005; Weber, 2007; Xiong et al., 2013) and human (For review: Bigler, 2013; Hulkower et al., 2013; Ng et al., 2014; Orrison et al., 2009) neuroimaging studies of repeated head trauma. Similar to the above studies, our study also found lower modulated

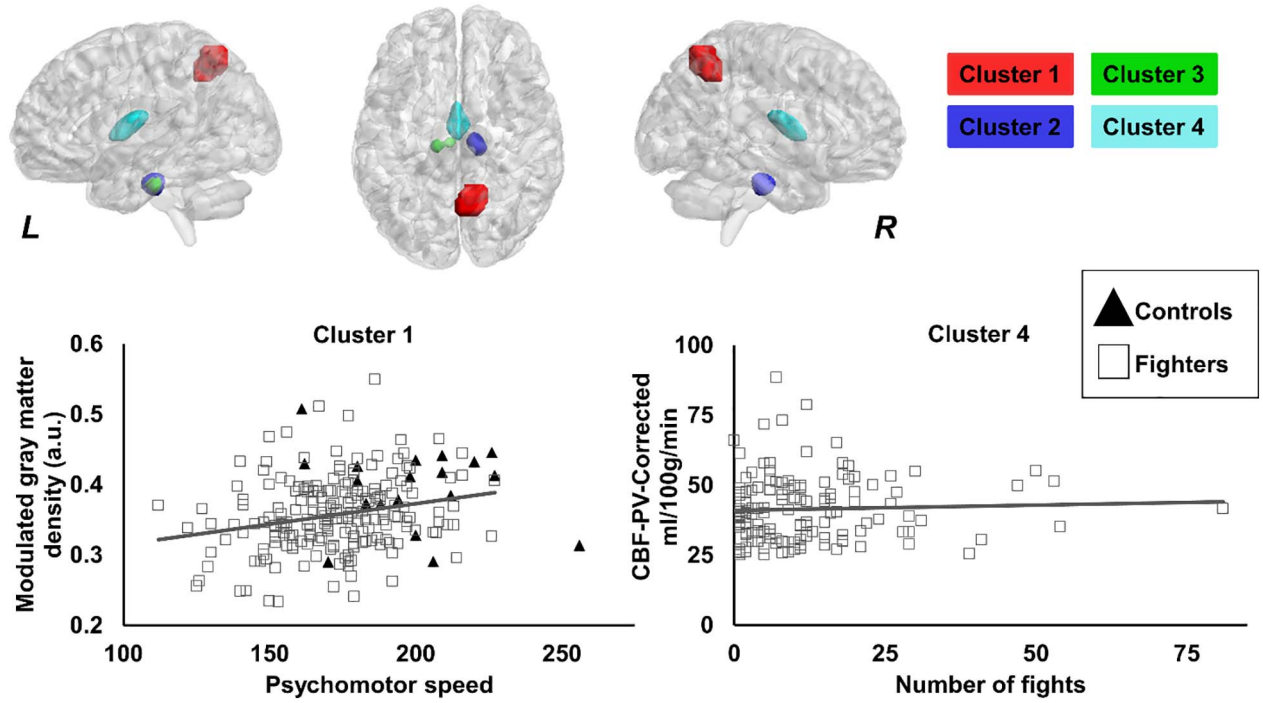


**Fig. 6.** Spatial location of the voxels where modulated GMD, WMD, and CBF-PV-Corr was different in fighters as compared to healthy controls. Cluster 1, cluster 2, cluster 3, and cluster 4 are shown in red, blue, green, and violet color respectively. The panel shows the 3D representation of the extent of the clusters from on MNI152 glass brain. L, R represents the left and right hemisphere. Scatterplot of CBF-PV-Corr is also shown as a function of psychomotor speed, and number of professional fights. Every scatter represents CBF-PV-Corr in the respective cluster for every subject. The regression line is shown for fighters in gray color. The regression line for controls is not shown as there was no association between CBF-PV-Corr and psychomotor speed. $*p < 0.05$. (For interpretation of the references to color in this figure legend, the reader is referred to the web version of this article.)

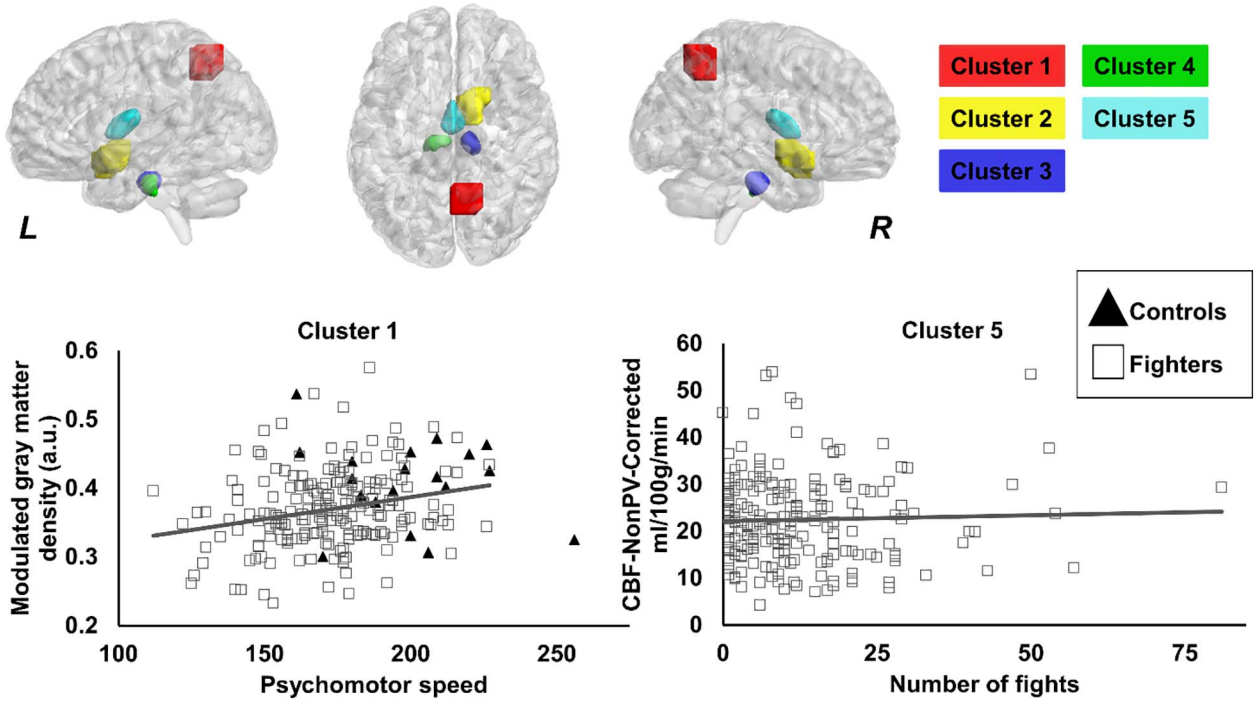


**Fig. 7.** Spatial location of the voxels where modulated GMD, WMD, and CBF-NonPV-Corr was different in fighters as compared to healthy controls. Cluster 1, cluster 2, cluster 3, cluster 4, and cluster 5 are shown in red, yellow, blue, green, and violet color respectively. The panel shows the 3D representation of the extent of the clusters from on MNI152 glass brain. L, R represents the left and right hemisphere. Scatterplot of CBF-NonPV-Corr is also shown as a function of psychomotor speed, and number of professional fights. Every scatter represents CBF-NonPV-Corr in the respective cluster for every subject. The regression line is shown for fighters in gray color. The regression line for controls is not shown as there was no association between CBF-NonPV-Corr and psychomotor speed. *$p < 0.05$. (For interpretation of the references to color in this figure legend, the reader is referred to the web version of this article.)

WMD in fighters as compared to healthy controls in pons, bilateral hippocampus and thalamus. WMD in thalamus was negatively associated with slower reaction time suggesting thalamus to be sensitive to repeated head trauma that has been speculated previously (Bernick et al., 2015).

Studies in retired fighters have also shown association of thalamic and hippocampal volumes with exposure to fighting and neuropsychological scores (Bernick et al., 2015; For review: Bigler, 2013; Koerte et al., 2016). However, we did not find any association of regional WMD deficits with exposure to fighting which may suggest that these structures may lack sensitivity to exposure to fighting due to the heterogeneous impact of brain injuries and inherent repair mechanism of individual fighters. Future longitudinal evaluation of hippocampus and thalamus atrophy may clarify the sensitivity of these regional WMD deficits due to fighting exposure. Our study, also, did not find any regional GMD difference between controls and fighters suggesting that gray matter deficits may not be as sensitive as white matter deficits.

Contrary to the previous studies (Rodriguez et al., 1998; For review: Kinoshita, 2016; Nortje and Menon, 2004), our study did not find any global CBF (both PV-Corr and NonPV-Corr) difference between fighters and controls and neither an association of global CBF with exposure to fighting or neuropsychological scores. This finding suggests that perfusion measurements may not be very sensitive to repeated head trauma and the metabolic studies may shed more light on perfusion changes in active professional fighters.

Various animal (Xiong et al., 2013 (review); Yamakami and McIntosh, 2004) and human (For review: Kinoshita, 2016; Nortje and Menon, 2004; Rostami et al., 2014; Werner and Engelhard, 2007) neuroimaging studies have reported dysregulated CBF due to repeated head trauma (For review: Kinoshita, 2016; Nortje and Menon, 2004; Rostami et al., 2014; Werner and Engelhard, 2007). Direct mechanical forces to the head at the time of impact have shown to induce both primary and secondary injuries manifesting as abnormal brain metabolism, dysregulated intracranial pressure (ICP) or changes in cerebral perfusion pressure (CPP) (For review: Hovda and Glenn, 2014; Kinoshita, 2016; Rangel-Castilla et al., 2008; Rose et al., 1977; Rostami et al., 2014). Dysregulated CBF is primarily caused due to uncoupling between flow and metabolism (Rostami et al., 2014 (review)). Factors leading to uncoupling between metabolism and flow such as cerebral vasospasm (Werner and Engelhard, 2007 (review)), cerebral metabolic

**Table 3**
Results of voxelwise modulated white matter density (WMD), partial volume corrected cerebral blood flow (CBF-PV-Corr), and non-partial volume corrected cerebral blood flow (CBF-NonPV-Corr) comparisons between controls and fighters are shown. The results were thresholded at cluster defining threshold (CDT) of $p < 0.001$ uncorrected. A family wise error rate at corrected $p < 0.05$ was applied and the clusters surviving the threshold for each group are tabulated. The extent of the cluster, mean ± SD for the compared group in the significant cluster and the effect sizes are tabulated. Refer Figs. 3–5 for the location of the clusters.

| Cluster | Mean ± standard deviation (controls) | Mean ± standard deviation (fighters) | Number of voxels in the cluster | Effect size |
|---|---|---|---|---|
| Modulated white matter density (a.u.) | | | | |
| Cluster 1 | 0.51 ± 0.05 | 0.49 ± 0.05 | 3534 | 0.89 ± 0.11 |
| CBF-PV-Corr (ml/100 g/min) | | | | |
| Cluster 1 | 65.45 ± 22.24 | 46.9 ± 14.93 | 194 | 0.89 ± 0.11 |
| CBF-NonPV-Corr (ml/100 g/min) | | | | |
| Cluster 1 | 35.22 ± 12.18 | 25.91 ± 7.99 | 263 | 0.91 ± 0.1 |
| Cluster 2 | 19.46 ± 12.56 | 29.52 ± 13.03 | 321 | 0.84 ± 0.06 |

**Table 4**
Multivariate results of voxelwise modulated gray matter density (GMD), white matter density (WMD), and partial volume corrected cerebral blood flow (CBF-PV-Corr) comparisons between controls and fighters are shown. A family wise error rate at corrected $p < 0.05$ was applied and the clusters surviving the threshold for each group are tabulated. The extent of the cluster, mean ± SD for the compared group in the significant cluster and the effect sizes are tabulated. Refer Fig. 6 for the location of the clusters.

| Cluster | Mean ± standard deviation (controls) | Mean ± standard deviation (fighters) | Number of voxels in the cluster | Canonical correlation (effect size) |
|---|---|---|---|---|
| Modulated gray matter density (a.u.) | | | | |
| Cluster 1 | 0.39 ± 0.06 | 0.36 ± 0.05 | | |
| Cluster 2 | 0.13 ± 0.02 | 0.12 ± 0.01 | | |
| Cluster 3 | 0.1 ± 0.01 | 0.09 ± 0.01 | | |
| Cluster 4 | 0.27 ± 0.03 | 0.26 ± 0.03 | | |
| Modulated white matter density (a.u.) | | | | |
| Cluster 1 | 0.31 ± 0.05 | 0.27 ± 0.05 | 104 | 0.28 ± 0.02 |
| Cluster 2 | 0.45 ± 0.05 | 0.42 ± 0.04 | 104 | 0.29 ± 0.02 |
| Cluster 3 | 0.53 ± 0.07 | 0.51 ± 0.05 | 80 | 0.28 ± 0.01 |
| Cluster 4 | 0.22 ± 0.03 | 0.2 ± 0.03 | 387 | 0.29 ± 0.03 |
| CBF-PV-Corr (ml/100 g/min) | | | | |
| Cluster 1 | 67.21 ± 21.55 | 61.07 ± 19.14 | | |
| Cluster 2 | 47.44 ± 18.79 | 50.89 ± 24.59 | | |
| Cluster 3 | 60.88 ± 26.42 | 58.18 ± 22.65 | | |
| Cluster 4 | 37.09 ± 14.83 | 33.2 ± 15.35 | | |

dysfunction (Rangel-Castilla et al., 2008 (review)), and presence of reactive oxygen species (van Mook et al., 2005 (review)) have been reported in various studies of different forms of brain injuries in human subjects, animal models and ex-vivo studies (Clausen et al., 2001; Lifshitz et al., 2003; Nortje and Menon, 2004 (review); Werner and Engelhard, 2007 (review); Yamakami and McIntosh, 2004).

Consistent with previous SPECT and ASL based CBF measurements that have reported hypoperfusion in temporal and parietal lobes, basal ganglia, thalamus, and cerebellum in various forms of repeated head trauma (Eierud et al., 2014; Koerte et al., 2016), our study also found lower CBF in the right inferior temporal lobes along with a paradoxical increase in CBF in the regions encompassing right cerebellum and right fusiform gyrus. The paradoxical increase of CBF in fighters vanished when CBF was corrected for partial volume correction. This finding may suggest that CBF increase due to repeated head trauma has to be discussed in light of structural morphology in the regions. Moreover, lack of association of CBF in temporal lobe with various neuropsychological assessments in fighters, which was found in controls, may suggest mismatch between CBF and oxygen extraction fraction (OEF) due to repeated head trauma. Since this study cannot measure OEF, it is imperative for future studies to study the effect of OEF on CBF. A longitudinal follow-up of the fighters with simultaneous metabolic studies will give a better insight about the evolution and mechanisms of CBF dysregulation in due to repeated head trauma.

Nonparametric multivariate analysis combining GMD and WMD with either CBF-PV-Corr or CBF-NonPV-Corr was conducted to further evaluate whether the findings reflect the changes due to repeated head trauma. Most of the cluster were similar to univariate analysis. However, an additional cluster in the right precuneus was revealed with multivariate analysis. In this cluster, modulated GMD was positively associated with psychomotor speed in fighters. Right precuneus has been shown to be involved with episodic memory (Cavanna and Trimble, 2006) and our finding may suggest that atrophy of the precuneus may be involved with cognition in our cohort of professional fighters. Also, the cluster in bilateral thalamus was positively associated with number of fights. Increase in CBF due to exposure to fighting may

**Table 5**
Multivariate results of voxelwise modulated gray matter density (GMD), white matter density (WMD), and partial volume corrected cerebral blood flow (CBF-PV-Corr) comparisons between controls and fighters are shown. A family wise error rate at corrected $p < 0.05$ was applied and the clusters surviving the threshold for each group are tabulated. The extent of the cluster, mean ± SD for the compared group in the significant cluster and the effect sizes are tabulated. Refer Fig. 7 for the location of the clusters.

| Cluster | Mean ± standard deviation (controls) | Mean ± standard deviation (fighters) | Number of voxels in the cluster | Canonical correlation (effect size) |
|---|---|---|---|---|
| Modulated gray matter density (a.u.) | | | | |
| Cluster 1 | 0.41 ± 0.06 | 0.37 ± 0.06 | | |
| Cluster 2 | 0.42 ± 0.04 | 0.41 ± 0.03 | | |
| Cluster 3 | 0.13 ± 0.01 | 0.12 ± 0.01 | | |
| Cluster 4 | 0.11 ± 0.01 | 0.1 ± 0.01 | | |
| Cluster 5 | 0.27 ± 0.03 | 0.26 ± 0.03 | | |
| Modulated white matter density (a.u.) | | | | |
| Cluster 1 | 0.3 ± 0.05 | 0.26 ± 0.05 | 69 | 0.3 ± 0.02 |
| Cluster 2 | 0.24 ± 0.03 | 0.24 ± 0.02 | 134 | 0.3 ± 0.02 |
| Cluster 3 | 0.46 ± 0.05 | 0.43 ± 0.05 | 147 | 0.28 ± 0.02 |
| Cluster 4 | 0.48 ± 0.06 | 0.46 ± 0.05 | 183 | 0.27 ± 0.01 |
| Cluster 5 | 0.22 ± 0.03 | 0.21 ± 0.03 | 365 | 0.3 ± 0.03 |
| CBF-NonPV-Corr (ml/100 g/min) | | | | |
| Cluster 1 | 42.99 ± 12.43 | 38.46 ± 11.74 | | |
| Cluster 2 | 52.81 ± 14.08 | 42.05 ± 12.59 | | |
| Cluster 3 | 30.15 ± 11.94 | 32.05 ± 13.74 | | |
| Cluster 4 | 33.42 ± 11.63 | 31.27 ± 11.47 | | |
| Cluster 5 | 23.66 ± 7.92 | 22.46 ± 9.43 | | |

**Table 6**
Summary of the univariate and multivariate findings in our cohort of active professional fighters and healthy controls.

| Statistical method used | Regions found to be significant | Associated with neuropyschological assessments or exposure to fighting |
|---|---|---|
| Univariate | | |
| ■ Structural MRI | | |
| a. Global gray matter density (GMD) | No difference | Positively associated with psychomotor speed in active professional fighters |
| b. Global white matter density (WMD) | No difference | Negatively associated with reaction time in active professional fighters |
| c. GMD (voxelwise) | No difference | No association |
| d. WMD (voxelwise) | Cluster involving bilateral pons, hippocampus, and thalamus | Negatively associated with reaction time in active professional fighters |
| ■ Cerebral blood flow (CBF) | | |
| a. Global Partial volume corrected (PV-Corr) | No difference | No association |
| b. Global Non-partial volume corrected (NonPV-Corr) | No difference | No association |
| c. PV-Corr (voxelwise) | Cluster in right inferior temporal lobe | Positively associated with verbal memory and negatively associated with reaction time in healthy controls |
| d. NonPV-Corr (voxelwise) | 1. Cluster in right inferior temporal lobe<br>2. Cluster in right fusiform gyrus and cerebellum | Positively associated with verbal memory and negatively associated with psychomotor speed and reaction time in healthy controls<br>No association |
| Multivariate voxelwise analysis | | |
| ■ GMD, WMD, and CBF-PV-Corr | 1. Cluster in right precuneus<br>2. Cluster in right hippocampus<br>3. Cluster in left hippocampus<br>4. Cluster in bilateral thalamus | Positively associated with psychomotor speed in healthy controls<br>No association<br>No association<br>Positively associated with number of professional fights |
| ■ GMD, WMD, and CBF-NonPV-Corr | 1. Cluster in right precuneus<br>2. Cluster in right olfactory cortex<br>3. Cluster in right hippocampus<br>4. Cluster in left hippocampus<br>5. Cluster in bilateral thalamus | Positively associated with psychomotor speed in healthy controls<br>No association<br>No association<br>No association<br>Positively associated with number of professional fights |

indicate reduced OEF to meet the increased metabolic demands, as mentioned above. These two findings may suggest that repeated head trauma induces complex heterogeneous pattern, both in perfusion and structural MRI measurements, and that a combined analysis of structural and perfusion measurements in addition to metabolic studies will help the clinicians better understand the pathophysiology of repeated head trauma.

However, the findings of our study have to be discussed with the following limitations. There was a mismatch in sample size and gender in our cohort of healthy controls and fighters population. Future studies with equal sampling of both genders should be performed to investigate differences due to repeated head trauma. Although statistically the controls are expected to have a low variance in both structural and CBF measures and similar performance on cognitive scores; future studies with equal distribution of sample sizes may be performed that can increase the power of interpretation of our study. A longitudinal analysis of active professional fighters will better reveal the pathophysiology of brain structure and perfusion due to repeated head impact as it is still unclear that the results of our analysis revealed structural and perfusion deficits due to repeated head impact. Our study was designed before the general consensus on ASL acquisition was published and hence the post labeling delay is shorter than the recommended value. We also assumed same arterial transit time (ATT) for fighters and healthy controls (Jain et al., 2012). It has been shown that ATT can vary in pathological cases (Grade et al., 2015; Yoshiura et al., 2009). Future studies should be designed to study the effect of repeated head trauma on ATT. Our simplest approach of partial volume correction with a fixed assumption of GM to WM ratio (Du et al., 2006) might not hold in the pathological brain. Although linear regression algorithms employed for partial volume correction (Asllani et al., 2008) with a single TI does not have this assumption, it is prone to smoothing which might reduce the chances of detecting localized changes (Ahlgren et al., 2014; Borogovac and Asllani, 2012). Future studies of perfusion quantification in subjects exposed to repeated head trauma should be evaluated using multiple post-labeling delay time as it has been shown to improve the repeatability of perfusion quantification (Zhao et al., 2017). Future studies should also be designed to simultaneously study CBV and CBF that can disentangle the role of repeated head trauma on CBV through hypercapnia (Ito et al., 2003; Pollock et al., 2009) or caffeine challenges (Addicott et al., 2009). Although none of the participants indicated hypertension, diabetes, or any other medical complications that may have influenced CBF (Novak, 2012), future studies could be directed to study the association of CBF and the role of other medical conditions influencing the clinical effects observed due to repeated head trauma in fighters. Since duration of knockouts could also influence CBF, future studies may also be directed to study the association of CBF and duration of knockouts in fighters (Barlow et al., 2016; Churchill et al., 2016). Although there was a medium to large effect (average Cohen's $d = 0.8$) in the regions with significant CBF deficits in fighters, there were no significant associations between CBF deficits and exposure to fighting or neuropsychological scores. Hence any clinical or physiological impact of this finding is unknown. Future studies will be directed towards investigating the association of the regions with lower CBF and cognition in fighters population. Furthermore, association of either structural or perfusion measurements in our cohort of active professional fighters does not imply causation.

## 5. Conclusion

In conclusion, our study found heterogeneous pattern of structural and CBF deficits due to repeated head trauma in active professional fighters. Heterogeneous loci of regional structural and CBF deficits were also observed but were not sensitive to fighting exposure. Multivariate analysis of structural and perfusion measurements revealed clusters where exposure to fighting was associated with deficits due to repeated head trauma. Overall, our finding suggests investigation of both structural and CBF deficits in same set of participants to understand the pathophysiology and progression of cognitive decline due to repeated head trauma.

## Acknowledgements

We would like to extend our sincere thanks to all the participants of the study, various research coordinators and MRI technologists without

which the study would not have been completed. We would also like to thank Dr. Mark Lowe and Dr. Wanyong Shin from Cleveland Clinic for their assistance in setting up the MRI protocols at our center and Dr. Anderson Winkler for the assistance on performing multivariate analysis. The funding sources have no role in the study design, data collection, data analysis, interpretation or writing of this article. All the authors had unrestricted access to the data in the study and had final decision to submit for publication.

## Funding

This work was supported by an Institutional Development Award (IDeA) from the National Institute of General Medical Sciences of the National Institutes of Health under grant number 5P20GM109025 and Lincy foundation.

## Declaration of interest

The authors declare no conflict of interest.

## References

Addicott, M.A., Yang, L.L., Peiffer, A.M., Burnett, L.R., Burdette, J.H., Chen, M.Y., Hayasaka, S., Kraft, R.A., Maldjian, J.A., Laurienti, P.J., 2009. The effect of daily caffeine use on cerebral blood flow: how much caffeine can we tolerate? Hum. Brain Mapp. 30, 3102–3114.

Ahlgren, A., Wirestam, R., Petersen, E.T., Ståhlberg, F., Knutsson, L., 2014. Partial volume correction of brain perfusion estimates using the inherent signal data of time-resolved arterial spin labeling. NMR Biomed. 27, 1112–1122.

Alsop, D.C., Detre, J.A., Golay, X., Günther, M., Hendrikse, J., Hernandez-Garcia, L., Lu, H., MacIntosh, B.J., Parkes, L.M., Smits, M., van Osch, M.J.P., Wang, D.J.J., Wong, E.C., Zaharchuk, G., 2015. Recommended implementation of arterial spin-labeled perfusion MRI for clinical applications: a consensus of the ISMRM perfusion study group and the European consortium for ASL in dementia. Magn. Reson. Med. 73, 102–116.

Ashburner, J., 2007. A fast diffeomorphic image registration algorithm. NeuroImage 38, 95–113.

Asllani, I., Borogovac, A., Brown, T.R., 2008. Regression algorithm correcting for partial volume effects in arterial spin labeling MRI. Magn. Reson. Med. 60, 1362–1371. http://dx.doi.org/10.1002/mrm.21670.

Barlow, K., Marcil, L.D., Carlson, H.L., Dewey, D., MacMaster, F.P., Brooks, B.L., Lebel, M., 2016. Cerebral perfusion changes in post-concussion syndrome: a prospective controlled cohort study. J. Neurotrauma 9, 1–9.

Bazarian, J.J., Cernak, I., Noble-Haeusslein, L., Potolicchio, S., Temkin, N., 2009. Long-term neurologic outcomes after traumatic brain injury. J. Head Trauma Rehabil. 24, 439–451.

Bernick, C., Banks, S., 2013. What boxing tells us about repetitive head trauma and the brain. Alzheimers Res. Ther. 5, 23.

Bernick, C., Banks, S., Phillips, M., Lowe, M., Shin, W., Obuchowski, N., Jones, S., Modic, M., 2013. Professional fighters brain health study: rationale and methods. Am. J. Epidemiol. 178, 280–286.

Bernick, C., Banks, S.J., Shin, W., Obuchowski, N., Butler, S., Noback, M., Phillips, M., Lowe, M., Jones, S., Modic, M., 2015. Repeated head trauma is associated with smaller thalamic volumes and slower processing speed: the Professional Fighters' Brain Health Study. Br. J. Sports Med. 49, 1007–1011.

Bigler, E.D., 2013. Traumatic brain injury, neuroimaging, and neurodegeneration. Front. Hum. Neurosci. 7, 395.

Blennow, K., Hardy, J., Zetterberg, H., 2012. The neuropathology and neurobiology of traumatic brain injury. Neuron 76, 886–899.

Borogovac, A., Asllani, I., 2012. Arterial Spin Labeling (ASL) fMRI: advantages, theoretical constrains, and experimental challenges in neurosciences. Int. J. Biomed. Imaging 2012, 818456.

Buxton, R.B., Frank, L.R., Wong, E.C., Siewert, B., Warach, S., Edelman, R.R., 1998. A general kinetic model for quantitative perfusion imaging with arterial spin labeling. Magn. Reson. Med. 40, 383–396.

Cavanna, A.E., Trimble, M.R., 2006. The precuneus: a review of its functional anatomy and behavioural correlates. Brain 129, 564–583. http://dx.doi.org/10.1093/brain/awl004.

Chappell, M.A., Groves, A.R., Whitcher, B., Woolrich, M.W., 2009. Variational Bayesian inference for a nonlinear forward model. IEEE Trans. Signal Process. 57, 223–236.

Chen, Y., Wolk, D.A., Reddin, J.S., Korczykowski, M., Martinez, P.M., Musiek, E.S., Newberg, A.B., Julin, P., Arnold, S.E., Greenberg, J.H., Detre, J.A., 2011. Voxel-level comparison of arterial spin-labeled perfusion MRI and FDG-PET in Alzheimer disease. Neurology 77, 1977–1985. http://dx.doi.org/10.1212/WNL.0b013e31823a0ef7.

Churchill, N., Hutchison, M., Richards, D., Leung, G., Graham, S., Schweizer, T.A., 2016. Brain structure and function associated with a history of sport concussion: a multimodal magnetic resonance imaging study. J. Neurotrauma 7 (neu.2016.4531).

Clausen, T., Zauner, A., Levasseur, J., Rice, A., Bullock, R., 2001. Induced mitochondrial failure in the feline brain: implications for understanding acute post-traumatic metabolic events. Brain Res. 908, 35–48.

Davis, A.E., 2000. Mechanisms of traumatic brain injury: biomechanical, structural and cellular considerations. Crit. Care Nurs. Q. 23, 1–13.

Du, A.T., Jahng, G.H., Hayasaka, S., Kramer, J.H., Rosen, H.J., Gorno-Tempini, M.L., Rankin, K.P., Miller, B.L., Weiner, M.W., Schuff, N., 2006. Hypoperfusion in frontotemporal dementia and Alzheimer disease by arterial spin labeling MRI. Neurology 67, 1215–1220. http://dx.doi.org/10.1212/01.wnl.0000238163.71349.78.

Eierud, C., Craddock, R., Fletcher, S., Aulakh, M., King-Casas, B., Kuehl, D., LaConte, S., 2014. Neuroimaging after mild traumatic brain injury: review and meta-analysis. NeuroImage. Clin. 4, 283–294.

Ge, Y., Patel, M.B., Chen, Q., Grossman, E.J., Zhang, K., Miles, L., Babb, J.S., Reaume, J., Grossman, R.I., 2009. Assessment of thalamic perfusion in patients with mild traumatic brain injury by true FISP arterial spin labelling MR imaging at 3T. Brain Inj. 23, 666–674.

Good, C.D., Johnsrude, I., Ashburner, J., Henson, R.N., Friston, K.J., Frackowiak, R.S., 2001. Cerebral asymmetry and the effects of sex and handedness on brain structure: a voxel-based morphometric analysis of 465 normal adult human brains. NeuroImage 14, 685–700.

Gooijers, J., Chalavi, S., Beeckmans, K., Michiels, K., Lafosse, C., Sunaert, S., Swinnen, S., 2013. Subcortical volume loss in the thalamus, putamen, and pallidum, induced by traumatic brain injury, is associated with motor performance deficits. Neurorehabil. Neural Repair 30, 603–614.

Grade, M., Hernandez Tamames, J.A., Pizzini, F.B., Achten, E., Golay, X., Smits, M., 2015. A neuroradiologist's guide to arterial spin labeling MRI in clinical practice. Neuroradiology 57, 1181–1202.

Graham, R., Rivara, F.P., Ford, M.A., Spicer, C.M. (Eds.), 2014. Sports-related Concussions in Youth: Improving the Science, Changing the Culture. National Academies Press (US), Washington (DC).

Gualtieri, C.T., Johnson, L.G., 2006. Reliability and validity of a computerized neurocognitive test battery, CNS vital signs. Arch. Clin. Neuropsychol. 21, 623–643.

Hall, E.D., Sullivan, P.G., Gibson, T.R., Pavel, K.M., Thompson, B.M., Scheff, S.W., 2005. Spatial and temporal characteristics of neurodegeneration after controlled cortical impact in mice: more than a focal brain injury. J. Neurotrauma 22, 252–265.

Hanyu, H., Sato, T., Shimizu, S., Kanetaka, H., Iwamoto, T., Koizumi, K., 2008. The effect of education on rCBF changes in Alzheimer's disease: a longitudinal SPECT study. Eur. J. Nucl. Med. Mol. Imaging 35, 2182–2190.

Heilbronner, R.L., Bush, S.S., Ravdin, L.D., Barth, J.T., Iverson, G.L., Ruff, R.M., Lovell, M.R., Barr, W.B., Echemendia, R.J., Broshek, D.K., 2009. Neuropsychological consequences of boxing and recommendations to improve safety: a National Academy of Neuropsychology education paper. Arch. Clin. Neuropsychol. 24, 11–19.

Herscovitch, P., Raichle, M.E., 1985. What is the correct value for the brain–blood partition coefficient for water? J. Cereb. Blood Flow Metab. 5, 65–69.

Hovda, D.A., Glenn, T.C., 2014. Human cerebral blood flow and traumatic brain injury. In: Lo, H.E., Lok, J., Ning, M., Whalen, J.M. (Eds.), Vascular Mechanisms in CNS Trauma. Springer New York, New York, NY, pp. 47–54.

Hulkower, M.B., Poliak, D.B., Rosenbaum, S.B., Zimmerman, M.E., Lipton, M.L., 2013. A decade of DTI in traumatic brain injury: 10 years and 100 articles later. AJNR Am. J. Neuroradiol. 34, 2064–2074.

Ito, H., Kanno, I., Ibaraki, M., Hatazawa, J., Miura, S., 2003. Changes in human cerebral blood flow and cerebral blood volume during hypercapnia and hypocapnia measured by positron emission tomography. J. Cereb. Blood Flow Metab. 23, 665–670.

Jain, V., Duda, J., Avants, B., Giannetta, M., Xie, S., Roberts, T., Detre, J., Hurt, H., Wehrli, F., Wang, D., 2012. Longitudinal reproducibility and accuracy of pseudo-continuous arterial spin-labeled perfusion MR imaging in typically developing children. Radiology 263, 527–536.

Jenkinson, M., Bannister, P., Brady, M., Smith, S., 2002. Improved optimization for the robust and accurate linear registration and motion correction of brain images. NeuroImage 17, 825–841.

Jordan, B.D., 2013. The clinical spectrum of sport-related traumatic brain injury. Nat. Rev. Neurol. 9, 222–230.

Kinoshita, K., 2016. Traumatic brain injury: pathophysiology for neurocritical care. J. Intensive Care 4, 29.

Koerte, I.K., Hufschmidt, J., Muehlmann, M., Lin, A.P., Shenton, M.E., 2016. Advanced Neuroimaging of Mild Traumatic Brain Injury, in: Laskowitz, D., Grant, G. Eds., Boca Raton (FL).

Langlois, J.A., Rutland-Brown, W., Wald, M.M., 2006. The epidemiology and impact of traumatic brain injury: a brief overview. J. Head Trauma Rehabil. 21, 375–378.

Leenders, K.L., Perani, D., Lammertsma, A.A., Heather, J.D., Buckingham, P., Healy, M.J., Gibbs, J.M., Wise, R.J., Hatazawa, J., Herold, S., 1990. Cerebral blood flow, blood volume and oxygen utilization. Normal values and effect of age. Brain 113, 27–47 (Pt 1).

Lifshitz, J., Friberg, H., Neumar, R., Raghupathi, R., Welsh, F., Janmey, P., Saatman, K., Wieloch, T., Grady, M., McIntosh, T., 2003. Structural and functional damage sustained by mitochondria after traumatic brain injury in the rat: evidence for differentially sensitive populations in the cortex and hippocampus. J. Cereb. Blood Flow Metab. 23, 219–231.

Liu, J., Liu, Y., Ren, L.-H., Li, L., Wang, Z., Liu, S.-S., Li, S.-Z., Cao, T.-S., 2016. Effects of race and sex on cerebral hemodynamics, oxygen delivery and blood flow distribution in response to high altitude. Sci. Rep. 6, 30500.

Liu, W., Wang, B., Wolfowitz, R., Yeh, P.-H., Nathan, D.E., Graner, J., Tang, H., Pan, H., Harper, J., Pham, D., Oakes, T.R., French, L.M., Riedy, G., 2013. Perfusion deficits in patients with mild traumatic brain injury characterized by dynamic susceptibility contrast MRI. NMR Biomed. 26, 651–663.

Lopez-Larson, M., King, J., McGlade, E., Bueler, E., Stoeckel, A., Epstein, D., Yurgelun-Todd, D., 2013. Enlarged thalamic volumes and increased fractional anisotropy in the thalamic radiations in veterans with suicide behaviors. Front. Psych. 4, 83.

Lu, H., Clingman, C., Golay, X., van Zijl, P.C.M., 2004. Determining the longitudinal relaxation time (T1) of blood at 3.0 Tesla. Magn. Reson. Med. 52, 679–682.
Margulies, S., Hicks, R., 2009 Jun. Combination therapies for traumatic brain injury: prospective considerations. J. Neurotrauma 26 (6), 925–939.
McKee, A.C., Cantu, R.C., Nowinski, C.J., Hedley-Whyte, E.T., Gavett, B.E., Budson, A.E., Santini, V.E., Lee, H.-S., Kubilus, C.A., Stern, R.A., 2009. Chronic traumatic encephalopathy in athletes: progressive tauopathy following repetitive head injury. J. Neuropathol. Exp. Neurol. 68, 709–735.
McKee, A.C., Stern, R.A., Nowinski, C.J., Stein, T.D., Alvarez, V.E., Daneshvar, D.H., Lee, H.-S., Wojtowicz, S.M., Hall, G., Baugh, C.M., Riley, D.O., Kubilus, C.A., Cormier, K.A., Jacobs, M.A., Martin, B.R., Abraham, C.R., Ikezu, T., Reichard, R.R., Wolozin, B.L., Budson, A.E., Goldstein, L.E., Kowall, N.W., Cantu, R.C., 2013. The spectrum of disease in chronic traumatic encephalopathy. Brain 136, 43–64.
Montenigro, P.H., Bernick, C., Cantu, R.C., 2015. Clinical features of repetitive traumatic brain injury and chronic traumatic encephalopathy. Brain Pathol. 25, 304–317.
Ng, T.S.C., Lin, A.P., Koerte, I.K., Pasternak, O., Liao, H., Merugumala, S., Bouix, S., Shenton, M.E., 2014. Neuroimaging in repetitive brain trauma. Alzheimers Res. Ther. 6, 10.
Nortje, J., Menon, D., 2004. Traumatic brain injury: physiology, mechanisms, and outcome. Curr. Opin. Neurol. 17.
Novak, V., 2012. Cognition and hemodynamics. Curr. Cardiovasc. Risk Rep. 6, 380–396.
Orrison, W.W., Hanson, E.H., Alamo, T., Watson, D., Sharma, M., Perkins, T.G., Tandy, R.D., 2009. Traumatic brain injury: a review and high-field MRI findings in 100 unarmed combatants using a literature-based checklist approach. J. Neurotrauma 26, 689–701.
Pollock, J.M., Deibler, A.R., Whitlow, C.T., Tan, H., Kraft, R.A., Burdette, J.H., Maldjian, J.A., 2009. Hypercapnia-induced cerebral hyperperfusion: an underrecognized clinical entity. AJNR Am. J. Neuroradiol. 30, 378–385.
Rangel-Castilla, L., Gasco, J., Nauta, H., Okonkwo, D., Robertson, C., 2008. Cerebral pressure autoregulation in traumatic brain injury. Neurosurg. Focus. 25, E7.
Rodriguez, G., Vitali, P., Nobili, F., 1998. Long-term effects of boxing and judo-choking techniques on brain function. Ital. J. Neurol. Sci. 19, 367–372.
Rose, J., Valtonen, S., Jennett, B., 1977. Avoidable factors contributing to death after head injury. Br. Med. J. 2, 615–618.
Rostami, E., Engquist, H., Enblad, P., 2014. Imaging of cerebral blood flow in patients with severe traumatic brain injury in the neurointensive care. Front. Neurol. 5, 114.
Shin, W., Mahmoud, S.Y., Sakaie, K., Banks, S.J., Lowe, M.J., Phillips, M., Modic, M.T., Bernick, C., 2014. Diffusion measures indicate fight exposure-related damage to cerebral white matter in boxers and mixed martial arts fighters. Am. J. Neuroradiol. 35, 285–290.
van Mook, W.N.K.A., Rennenberg, R.J.M.W., Schurink, G.W., van Oostenbrugge, R.J., Mess, W.H., Hofman, P.A.M., de Leeuw, P.W., 2005. Cerebral hyperperfusion syndrome. Lancet Neurol. 4, 877–888.
Victoroff, J., 2013. Traumatic encephalopathy: review and provisional research diagnostic criteria. NeuroRehabilitation 32, 211–224.
Wang, Z., Aguirre, G.K., Rao, H., Wang, J., Fernández-Seara, M.A., Childress, A.R., Detre, J.A., 2008. Empirical optimization of ASL data analysis using an ASL data processing toolbox: ASLtbx. Magn. Reson. Imaging 26, 261–269.
Weber, J.T., 2007. Experimental models of repetitive brain injuries. Prog. Brain Res. 161, 253–261.
Werner, C., Engelhard, K., 2007. Pathophysiology of traumatic brain injury. Br. J. Anaesth. 99, 4–9.
Winkler, A.M., Ridgway, G.R., Douaud, G., Nichols, T.E., Smith, S.M., 2016. Faster permutation inference in brain imaging. NeuroImage 141, 502–516.
Wintermark, M., Sanelli, P.C., Anzai, Y., Tsiouris, A.J., Whitlow, C.T., 2015. Imaging evidence and recommendations for traumatic brain injury: advanced neuro- and neurovascular imaging techniques. AJNR Am. J. Neuroradiol. 36, E1–E11.
Worsley, K.J., Marrett, S., Neelin, P., Vandal, A.C., Friston, K.J., Evans, A.C., Square, Q., F, U.K.W.C.N.K.J., 1996. A unified statistical approach for determining significant signals in images of cerebral activation. Hum. Brain Mapp. 73.
Wu, W.-C., Fernandez-Seara, M., Detre, J.A., Wehrli, F.W., Wang, J., 2007. A theoretical and experimental investigation of the tagging efficiency of pseudocontinuous arterial spin labeling. Magn. Reson. Med. 58, 1020–1027.
Xiong, Y., Mahmood, A., Chopp, M., 2013. Animal models of traumatic brain injury. Nat. Rev. Neurosci. 14, 128–142.
Yamakami, I., McIntosh, T., 2004. Effects of traumatic brain injury on regional cerebral blood flow in rats as measured with radiolabeled microspheres. J. Cereb. Blood Flow Metab. 24, 202–211.
Yoshiura, T., Hiwatashi, A., Yamashita, K., Ohyagi, Y., Monji, A., Takayama, Y., Nagao, E., Kamano, H., Noguchi, T., Honda, H., 2009. Simultaneous measurement of arterial transit time, arterial blood volume, and cerebral blood flow using arterial spin-labeling in patients with Alzheimer disease. AJNR Am. J. Neuroradiol. 30, 1388–1393.
Zhang, L., Heier, L.A., Zimmerman, R.D., Jordan, B., Ulug, A.M., 2006. Diffusion anisotropy changes in the brains of professional boxers. AJNR Am. J. Neuroradiol. 27, 2000–2004.
Zhang, L., Ravdin, L.D., Relkin, N., Zimmerman, R.D., Jordan, B., Lathan, W.E., Uluğ, A.M., 2003. Increased diffusion in the brain of professional boxers: a preclinical sign of traumatic brain injury? AJNR Am. J. Neuroradiol. 24, 52–57.
Zhang, Y., Brady, M., Smith, S., 2001. Segmentation of brain MR images through a hidden Markov random field model and the expectation-maximization algorithm. IEEE Trans. Med. Imaging 20, 45–57.
Zhao, M.Y., Mezue, M., Segerdahl, A.R., Okell, T.W., Tracey, I., Xiao, Y., Chappell, M.A., 2017. A systematic study of the sensitivity of partial volume correction methods for the quantification of perfusion from pseudo-continuous arterial spin labeling MRI. NeuroImage 162, 384–397. http://dx.doi.org/10.1016/j.neuroimage.2017.08.072.